Hindawi Publishing Corporation
International Journal of Distributed Sensor Networks
Volume 2016, Article ID 9437602, 10 pages
http://dx.doi.org/10.1155/2016/9437602

Research Article

Sparsity-Based Optimization of the Sensors Positions in Radar Networks with Separated Transmit and Receive Nodes

I. M. Ivashko, O. A. Krasnov, and A. G. Yarovoy

Microwave Sensing, Systems and Signals (MS3), Delft University of Technology, Mekelweg 4, 2628 CD Delft, Netherlands

Correspondence should be addressed to I. M. Ivashko; i.ivashko@tudelft.nl

Received 18 September 2015; Revised 24 December 2015; Accepted 27 December 2015

Academic Editor: Shengming Jiang

A sparsity-based approach for the joint optimization of the transmit and the receive nodes positions in the radar network with widely distributed antennas is proposed in this paper. The optimization problem is formulated as minimization of the number of radars that meet fixed target localization requirements over the surveillance area. We demonstrated that this type of the problem is different from the problem of the monostatic radar network topology optimization and implies the bilinear matrix inequality (BMI) problem. To tackle it, we propose to use the relaxation technique, which allows for joint selection of the positions for transmit and receive radar nodes. Provided numerical analysis shows that, in order to satisfy the same requirements to the target localization accuracy, the radar network with bistatic radars requires less number of the nodes than the one with monostatic radars.

1. Introduction

The variety of applications of the radar (sensor) networks is constantly increasing in both civil and military domains. Such applications include homeland security and border control, environmental monitoring, and patient monitoring to list a few [1–3]. Availability of low-cost radars with wide-beam/omnidirectional antennas provides opportunity to estimate the target state vector over wide surveillance area using joint processing of data from widely distributed radar nodes. The spatial diversity of the radars allows for better resolution, higher detectability, and fault tolerance compared to a single conventional monostatic radar [4]. The costs of the system design, delivery, maintenance, and operation are lower for the radar networks as well.

Within a wide spectrum of the radar networks, particular systems differ from each other by (i) the way of radar interaction with the target of interest (active way, passive way, or combination of both), (ii) the level of the spatial coherency (nodes can be mutually coherent, with short time coherency, and noncoherent), (iii) the method of the information fusion from individual radar nodes (fusion of radio frequency signals, video signals, individual targets' detections and parameters measurements, and tracks), (iv) the level of autonomy in the signal reception and processing (autonomous level, cooperative level, or combination of both), and (v) the radar nodes architecture (monostatic radars, bistatic radars, or combination of both). These features and the parameters of the single radar define overall system performance [5]. For example, the network of multistatic radars with cooperative mode provides comparable estimation accuracy to the network of monostatic radars with autonomous reception mode, using two times less transmit/receive channels.

The topology of the radar nodes affects the system performance as well. For example, the target localization accuracy of the radar network is affected by the ranging errors of each radar [6]. In Global Positioning Systems, where the ranging errors of the different satellites are the same, this effect can be described with the Geometric Dilution of Precision (GDOP) factor. The GDOP is defined as a ratio of the localization error to the ranging error, which is the same for all satellites. In the network of radars, where the ranging accuracy will be different for each radar node, this effect is described with the Cramér-Rao Lower Bound (CRLB). In both systems, the best estimation can be achieved with symmetrical and balanced topology of the sensing nodes [7, 8].

However, in most of the applications, the available locations for the radar nodes are limited due to several reasons, such as the system cost, the availability of communication

links and their data rates, and the existing infrastructure. Therefore, one of the key issues of the effective exploitation of radar networks is providing optimal topology of the radar nodes in terms of (minimum) estimation error. In general, this problem can be formulated in two ways: (i) to find the minimum number of the radar nodes positions that guarantee predefined target localization accuracy and (ii) to find optimal positions for a fixed number of the radar nodes such that the target localization error is minimal.

The problem of the optimization of nodes positions of the sensor networks has been studied in the recent decades in both radar and communication fields [9–11]. In particular, the developed state-of-the-art techniques that are based on convex, greedy, and heuristic optimization can be exploited for different types of monostatic sensors [10–12]. Some of these techniques can be modified for the radar networks that use signals from transmitters of opportunity (passive bistatic radars (PBR)) [12, 13]. To the authors' knowledge, there is no work dedicated to the joint position optimization of the transmit and receive radar nodes in the radar networks that use dedicated transmitters. This type of the radar network is also known as *statistical* multiple-input multiple-output (MIMO) radar [4]. On the designing stage of the statistical MIMO radar the question of how to make the trade-off on devoting the available location either to transmit or receive nodes arises.

In this paper, we address the problem of joint optimization of the transmit (Tx) and receive (Rx) radar nodes positions in the radar networks with widely separated antennas. We formulate the generic optimization problem of the first type, where the optimal positions of Tx and Rx radar nodes have to be selected in order to meet fixed accuracy requirements to target localization. This optimization problem implies the bilinear matrix inequality (BMI). We relax it to the linear matrix inequality (LMI) by introducing new variables that describe each of the Tx-Rx channels of the radar network. We explore the sparsity-based algorithm introduced in [11] to solve this problem. The algorithm can be applied for the selection of the favorable radar nodes' positions in scenarios, where the conditions of network regularity and symmetry cannot be satisfied. Another advantage of this algorithm is its ability to find global minimum of the objective function in contrast to the heuristic optimization algorithms. We developed technique, based on the convex optimization, for the selection of the positions for transmitting and receiving radar nodes that satisfy given requirements to the estimation accuracy of the radar network. We applied the developed framework to the topology optimization of the Frequency-Modulated Continuous-Wave (FMCW) radar network with widely separated transmit and receive radar nodes. The corresponding theory on the evaluation of the target localization accuracy using the Fisher information matrix (FIM) has been developed.

The paper is organized as follows. The system model is introduced in Section 2. Section 3 provides the developed framework to the radar network topology optimization problem. The comparative numerical analysis of the radar network performance and topology optimization for different types of the systems is given in Section 4. In Appendix, the theoretical bounds on the target localization accuracy (Cramér-Rao Lower Bound) in Frequency-Modulated Continuous-Wave radar network are presented.

2. System Model

We consider an active radar network with N transmitting and M receiving nodes in 3D space. The Tx and Rx nodes can be either colocated or separated corresponding to the monostatic and bistatic radar architectures, respectively. In the model of bistatic radar network, it is assumed that each of N totally available transmitters forms a bistatic sensing pair with each of M available receivers that correspond to the cooperative mode of the signal reception and result in $J = NM$ bistatic radars, if not specified otherwise. In case of monostatic radar network, the number of Tx channels N is equal to the number of Rx channels M, which forms $J = N = M$ monostatic radars. Monostatic radars are assumed to use autonomous mode of the signal reception; that is, each of the receivers receives signal from the dedicated (colocated) transmitter.

Antenna patterns of the Tx and Rx antennas are assumed to be omnidirectional. The target detection is based on the reflected signal. The data fusion is made on the level of single measurements of the estimated signal parameters at each of the receiving radar nodes. This implies two-step algorithm of the target localization. The fist step includes target detection and estimation of the signal parameters. In the second step, the target position vector is evaluated by applying appropriate positioning algorithm. For example, for target localization using the set of the measured signal time delays, the multilateration algorithm, based on the direct calculation, can be applied [14]. The target localization in 2D plane with multilateration algorithm that uses two measured bistatic distances is shown in Figure 1. In 3D space, the coordinate surfaces correspond to the ellipsoids of revolution in the points of transmitting and receiving positions of bistatic radar.

We consider the following measurement model:

$$\mathbf{r} = \mathbf{f}(\boldsymbol{\psi}) + \boldsymbol{\xi}, \tag{1}$$

where $\mathbf{r} \in \mathbb{R}^J$ is the vector that represents accumulated measurements, namely, signal time delays, in J bistatic pairs; $\boldsymbol{\psi} = [x, y, z]$ is the parameter vector that represents the true target coordinates; $\mathbf{f}(\cdot)$ is the nonlinear function; $\boldsymbol{\xi}$ is the measurement noise. The nonlinear function $\mathbf{f}(\cdot)$ from (1) is the signal time delay measured in the jth bistatic radar and is related to the target and radar nodes' positions as follows:

$$\tau_j = \frac{R_n^{(t)} + R_m^{(r)}}{c}, \tag{2}$$

where c is the speed of light, and

$$\begin{aligned} R_n^{(t)} &= \sqrt{\left(x - x_n^{(t)}\right)^2 + \left(y - y_n^{(t)}\right)^2 + \left(z - z_n^{(t)}\right)^2}, \\ R_m^{(r)} &= \sqrt{\left(x - x_m^{(r)}\right)^2 + \left(y - y_m^{(r)}\right)^2 + \left(z - z_m^{(r)}\right)^2} \end{aligned} \tag{3}$$

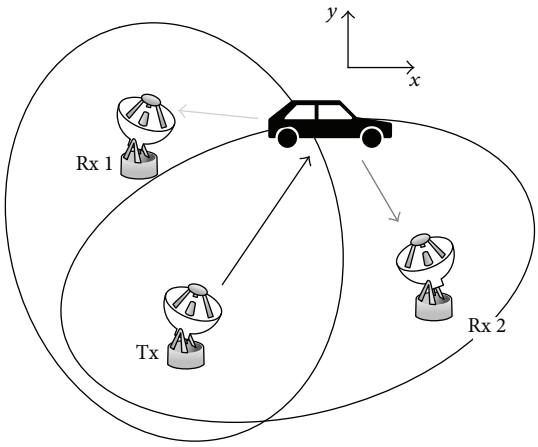

Figure 1: Target localization in multistatic radar network with cooperative mode of signal reception.

are distances from the nth transmitter and mth receiver to the target; $n = 1, \ldots, N$; $m = 1, \ldots, M$; $\mathbf{p} = [x \;\; y \;\; z]$ is the coordinate vector of the target, $\mathbf{p}_n^{(t)} = [x_n^{(t)}, y_n^{(t)}, z_n^{(t)}]$, and $\mathbf{p}_m^{(r)} = [x_m^{(r)}, y_m^{(r)}, z_m^{(r)}]$ are coordinate vectors of the nth transmitter and the mth receiver, respectively.

A single target case is considered throughout the paper. It is assumed that the measurements from the multiple targets in the scene are associated using appropriate data association algorithm, like the one presented in [15]. Effects of the signal multipath are neglected, assuming that multipath is suppressed during the detection and the estimation in a single radar. The signal attenuation that occurs due to the finite target-radar distance is taken into account, following the classic radar equation:

$$P_r = \frac{P_t G^{(t)} G^{(r)} \mathrm{RCS} \lambda^2}{(4\pi)^3 R_n^2 R_m^2 L_{\mathrm{syst}}} G_p, \tag{4}$$

where P_r is the received signal power, P_t is the transmitted power, $G^{(t)}$ is the Tx antenna gain, $G^{(r)}$ is the Rx antenna gain, RCS is the radar cross section, λ is the signal wavelength, L_{syst} is the system loss, and G_p is the processing gain.

3. Radar Network Geometry Optimization

We use the Cramér-Rao Lower Bound (the inverse of the Fisher information matrix) as the performance metric of the system to evaluate the target localization accuracy. Although the CRLB approaches the maximum likelihood estimatior (MLE) at high signal-to-noise ratios (SNR), it remains an effective metric of the radar network performance [16]. It incorporates the operational parameters of the single radar node as well as the system features (such as topology of the nodes, their architecture, and cooperation mode). Hence, the effect of these factors upon the system performance can be analyzed with the CRLB. Moreover, with increasing the number of the radar nodes, the threshold point (the point up to which the CRLB approaches the MLE asymptotically) moves to the lower SNR regions [17].

For unbiased estimator $\widehat{\boldsymbol{\theta}}$ of the parameter vector $\boldsymbol{\theta}$, the CRLB allows one to place a bound on the variance of each element from the parameter vector $\boldsymbol{\theta} = [\theta_1, \ldots, \theta_K]$ [18]:

$$\mathrm{Var}\left(\widehat{\theta}_i\right) \geq \left[\mathbf{I}^{-1}(\theta)\right]_{ii}, \tag{5}$$

where $\mathbf{I}$ is the $K \times K$ Fisher information matrix (FIM) with elements

$$[\mathbf{I}(\theta)]_{ij} = -\left\langle \frac{\partial^2 \ln g(\mathbf{r}; \boldsymbol{\theta})}{\partial\theta_i \partial\theta_j} \right\rangle, \tag{6}$$

where $g(\mathbf{r}; \boldsymbol{\theta})$ is the probability density function of the parameter vector $\boldsymbol{\theta}$; $\langle \cdots \rangle$ means statistical average of the quantity in the brackets; $i = 1, \ldots K$; $j = 1, \ldots K$.

One of the functions of the FIM can be used as metrics of the system estimation accuracy: the minimum eigenvalue ($\lambda_{\min}$), which indicates the length of the major axis of the error ellipsoid that corresponds to the maximum estimation error, the sum of the eigenvalues that corresponds to the sum of the errors, and the (log) determinant, which is the (log) volume of the confidence ellipsoid [11, 19, 20].

In the optimization algorithm, we constraint the minimum eigenvalue of the FIM $\lambda_{\min}$ with the threshold λ_g. This corresponds to the constraint on the localization error $\boldsymbol{\sigma}_{\mathrm{pos}} = \widetilde{\mathbf{p}} - \mathbf{p}$, which has to be within an origin-centered ellipsoid (in 3D space) with the longest axis R_e and probability higher than P_e: $\Pr(\|\boldsymbol{\sigma}_{\mathrm{pos}}\|_2 \leq R_e) \geq P_e$ [21]. For the parameter vector $\boldsymbol{\theta}$ with three components $K = 3$, the probability P_e is given by [6]

$$P_e(q) = \mathrm{erf}\left(\frac{\sqrt{q}}{2}\right) - \frac{\sqrt{2q}}{\pi} \exp\left(\frac{-q}{2}\right), \tag{7}$$

where

$$\mathrm{erf} = \frac{2}{\sqrt{\pi}} \int_0^x \exp\left(-t^2\right) dt \tag{8}$$

is the error function and q is the constant that determines the size of the confidence ellipsoid and relates to its semimajor axis as $R_e^2 = q\lambda_{\min}$.

3.1. The Radar Network with Colocated Transmit and Receive Antennas. We formulate the following optimization problem to select the minimum number $\widetilde{J}$ of sensing locations from the J available ones ($\widetilde{J} \ll J$) that allow for the target localization with predefined accuracy requirements from the target area S:

$$\begin{aligned} \min \quad & \mathbf{1}_J^T \mathbf{w} \\ \text{s.t.} \quad & \lambda_{\min} \mathbf{I}(\mathbf{w}) \geq \lambda_g, \quad \forall \mathbf{p} \in S \\ & w_j \in \{0, 1\}, \quad j = 1, \ldots, J, \end{aligned} \tag{9}$$

where the minimization of the cost function corresponds to the minimization of l_1-norm of the selection vector $\mathbf{w} \in \mathbb{R}^J$ with $w_j = 1(0)$ which indicates whether the jth candidate

position is selected or not; $\mathbf{I}$ is the Fisher information matrix on the target localization in the radar network:

$$\mathbf{I}(\mathbf{p}) = \sum_{j=1}^{J} [\mathbf{I}(\mathbf{p})]^{(j)} \tag{10}$$

with $\mathbf{I}^{(j)}$ being the FIM constructed, based on measurements from jth radar (example on construction of the FIM on target localization in FMCW radar network can be found in Appendix A).

The dependence of the target localization accuracy upon the selected radars is introduced using the multiplication of each of the FIMs $\mathbf{I}^{(j)}$ by corresponding value from the selection vector w_j:

$$\mathbf{I}(\mathbf{w}, \mathbf{p}) = \sum_{j=1}^{J} w_j [\mathbf{I}(\mathbf{p})]^{(j)}. \tag{11}$$

Problem (9) is a convex optimization problem that can be solved with the algorithm presented in [11] by minimizing the reweighted l_1-norm of the selection vector $\mathbf{w}$:

$$\min_{\mathbf{w} \in R^J} \quad \mathbf{u}^T \mathbf{w}, \tag{12}$$

where $\mathbf{u}$ is a weight vector with components $u_j^{(k)} = 1/(\epsilon + w_j^{(k)})$ updated in each of kth iterations; ϵ is a small number that prevents division by zero. The use of the weight vector $\mathbf{u}$ in the cost function allows for the smaller number of the radar positions to be selected, compared to l_1-norm minimization [22].

Since the number of the selected positions $\widetilde{J}$ is much less than the number of alternative ones $\widetilde{J} \ll J$, the selection vector $\mathbf{w}$ contains small number of the nonzero entries. These nonzero entries represent the number of radars required to reconstruct the target position vector with predefined estimation accuracy. In this manner, the optimization problem is sparse.

3.2. The Radar Network with Widely Separated Transmit and Receive Antennas

3.2.1. Problem Formulation. In this section we consider bistatic radar network with cooperative mode of the signal transmission reception; that is, signals scattered from the target due to illumination by all of the transmit radar nodes are received by all of the receiving radar nodes. Then the Fisher information matrix that characterizes the system performance can be represented as

$$\mathbf{I}\left(\mathbf{w}^{(t)}, \mathbf{w}^{(r)}, \mathbf{p}\right) = \sum_{n=1}^{N} \sum_{m=1}^{M} w_n^{(t)} w_m^{(r)} [\mathbf{I}(\mathbf{p})]^{(nm)}, \tag{13}$$

where $\mathbf{w}^{(t)}$ and $\mathbf{w}^{(r)}$ are the selection vectors of Tx and Rx radar nodes' positions.

In order to choose the favorable geometry of bistatic radars, the positions of transmitting N and receiving antennas M have to be optimized simultaneously. The minimization function is then a sum of two (reweighted) l_1-norms and the problem of the multistatic radar network geometry optimization is formulated as

$$\begin{aligned} \min_{\mathbf{w}^{(t)} \in R^N, \mathbf{w}^{(r)} \in R^M} \quad & \left(\left(\mathbf{u}^{(t)}\right)^T \mathbf{w}^{(t)} + \left(\mathbf{u}^{(r)}\right)^T \mathbf{w}^{(r)}\right) \\ \text{s.t.} \quad & \sum_{n=1}^{N} \sum_{m=1}^{M} w_n^{(t)} w_m^{(r)} [\mathbf{I}(\mathbf{p})]^{(nm)} - \lambda_g \mathbb{1}_3 \succeq 0, \\ & \forall \mathbf{p} \in S \\ & w_n^{(t)} \in \{0, 1\}, \quad n = 1, \ldots, N \\ & w_m^{(r)} \in \{0, 1\}, \quad m = 1, \ldots, M, \end{aligned} \tag{14}$$

where $\mathbf{u}^{(t)}$ and $\mathbf{u}^{(r)}$ are weight vectors for the number of Tx and Rx radar units with the elements $[u_n^{(t)}]^{(k)} = 1/(\epsilon + [w_n^{(t)}]^{(k)})$ and $[u_m^{(r)}]^{(k)} = 1/(\epsilon + [w_m^{(r)}]^{(k)})$, respectively. The notation $\mathbf{I} \succeq \mathbb{1}$ means that matrix $(\mathbf{I} - \mathbb{1})$ is positive semidefinite ($\mathbf{I}$ and $\mathbb{1}$ are symmetrical matrices).

Constraint in (14) implies the *bilinear matrix inequality* (BMI) problem. BMI problems are NP-hard and include all quadratic problems. There are local and global methods for the solution of BMI optimization problems. Local method implies an alternate optimization over the parameters $\mathbf{w}^{(t)}$ and $\mathbf{w}^{(r)}$. In the global method (branch-and-bound type) the solution can be found by relaxing BMI problem to the linear matrix inequality (LMI) problem. We apply semidefinite relaxation to solve the problem of the geometry optimization of multistatic radar networks.

3.2.2. Semidefinite Relaxation in BMI Problem of Multistatic Radar Network Geometry Optimization. First, we substitute the bilinear terms $w_n^{(t)}$ and $w_m^{(r)}$ in (14) with new variable $\boldsymbol{\gamma} = [w_1^{(t)}, \ldots, w_N^{(t)}, w_1^{(r)}, \ldots, w_M^{(r)}]^T$ and introduce the bound on γ_j [23]. Consequently, the optimization problem (14) will be

$$\begin{aligned} \min_{\mathbf{w}^{(t)} \in R^N, \mathbf{w}^{(r)} \in R^M} \quad & \left(\left(\mathbf{u}^{(t)}\right)^T \mathbf{w}^{(t)} + \left(\mathbf{u}^{(r)}\right)^T \mathbf{w}^{(r)}\right) \\ \text{s.t.} \quad & \sum_{n=1}^{N} \sum_{m=1}^{M} g_{nm} [\mathbf{I}(\mathbf{p})]^{(nm)} - \lambda \mathbb{1}_3 \succeq 0, \\ & \forall \mathbf{p} \in S \\ & g_{nm} = w_n^{(t)} w_m^{(r)}, \\ & n = 1, \ldots, N; \; m = 1, \ldots, M. \end{aligned} \tag{15}$$

Then we relax the constraint on g_{nm} as LMI:

$$\begin{aligned} \min_{\mathbf{w}^{(t)}\in R^N, \mathbf{w}^{(r)}\in R^M} \quad & \left(\left(\mathbf{u}^{(t)}\right)^T \mathbf{w}^{(t)} + \left(\mathbf{u}^{(r)}\right)^T \mathbf{w}^{(r)}\right) \\ \text{s.t.} \quad & \sum_{n=1}^{N}\sum_{m=1}^{M} g_{nm}\left[\mathbf{I}(\mathbf{p})\right]^{(nm)} - \lambda_g \mathbb{1}_3 \succeq 0, \\ & \qquad \forall \mathbf{p} \in S \\ & \begin{bmatrix} \mathbf{G} & \boldsymbol{\gamma} \\ \boldsymbol{\gamma}^T & 1 \end{bmatrix} \succeq 0, \quad \operatorname{diag}(\mathbf{G}) = \boldsymbol{\gamma} \end{aligned} \tag{16}$$

where $\mathbf{G} = \gamma\gamma^T$.

Problem (16) is a semidefinite programming (SDP) problem in the variables $\mathbf{G}$ and $\boldsymbol{\gamma}$. Similar to the monostatic radar network optimization [11], the optimization algorithm for the selection of the multistatic radar network topology is as follows:

(1) *Initialize* the iteration counter $k = 0$ and the weight vectors $\mathbf{u}^{(t)} = \mathbf{1}_N$, $\mathbf{u}^{(r)} = \mathbf{1}_M$.

(2) *Solve* the weighted l_1-norm minimization problem (16) for the optimum $\boldsymbol{\gamma}^{(k)}$ in the kth iteration.

(3) *Update* the weight vectors: $[u_n^{(t)}]^{(k)} = 1/(\epsilon + [w_n^{(t)}]^{(k)})$ and $[u_m^{(r)}]^{(k)} = 1/(\epsilon + [w_m^{(r)}]^{(k)})$ for each $n = 1, \ldots, N$ and $m = 1, \ldots, M$.

(4) *Stop* on convergence or when k attains a specified maximum number of iterations $k_{\max}$, otherwise, increment k and go to step (2).

The application of the relaxation technique leads to non-Boolean solution of the optimization problem. An approximate Boolean solution can be found by thresholding nonzero entries of the vector γ or by applying the randomization technique [24].

As one can see, the structure of the FIM that describes the target localization performance of the radar network is defined as one that incorporates the estimation performance of each radar (Tx-Rx channel) $\mathbf{I}^{(j)}$. The cooperation mode of the signal reception will result in higher number of Tx-Rx channels, compared to the autonomous mode of the signal reception. Therefore, as soon as the FIM of each Tx-Tx channel $\mathbf{I}^{(j)}$ in the radar network is defined, the target localization accuracy of the system can be easily evaluated. To summarize, the developed generic framework can be applied for the optimization of the radar nodes positions in the radar networks that consist of different types of the radar sensors, which can be both homogeneous and heterogeneous. In the next section, we present the application of the developed theory to the optimization of the radar nodes positions of the FMCW radar network.

4. Numerical Results

In this section, we present the comparative analysis of the potential localization accuracy of multistatic and monostatic FMCW radar networks with application of the topology optimization algorithm. It is assumed that transmitted signals are orthogonal and do not interfere with each other [25]. Free-space model of signal propagation is used, assuming that the line-of-sight signal corresponds to the first and the strongest signal component in time.

4.1. Signal Model. The reference linear frequency modulated (LFM) up-chirp signal is

$$s(t) = \exp\left[it\left(\omega_0 + \frac{\Delta\omega}{T_s}\left(t - (q-1)T_s\right)\right)\right], \tag{17}$$

where ω_0 is an angular frequency, related to the carrier frequency of the transmitted signal f_c as $\omega_0 = 2\pi f_c$; $\Delta\omega$ is an angular frequency bandwidth, related to the signal bandwidth Δf as $\Delta\omega = 2\pi\Delta f$; T_s is the duration of the single sawtooth pulse (sweep time); $q = 1, \ldots, Q$ denotes the pulse number with Q being the number of integrated train pulses used in signal processing for signal parameters estimation, $0 < t < QT_s$.

The signal, reflected from the point moving target, is

$$r(t) = |A| \exp(i\varphi)\, s(t - \tau, \omega_0 - \omega_d) + \xi(t), \tag{18}$$

where $|A|\exp(i\varphi)$ is the nonfluctuating complex signal amplitude; $\omega_d = 2\pi f_d$ is an angular Doppler frequency shift with f_d being the Doppler frequency; ξ is zero-mean Gaussian noise with variance $\sigma^2 : \xi \sim \mathcal{N}(0, 2\sigma^2)$.

In addition to the time delay and Doppler frequency, the complex amplitude $A\exp(i\varphi)$ of the received signal is measured as well. Consequently, the parameter vector contains four components $K = 4$: $\boldsymbol{\theta} = [\tau, \omega_d, |A|, \varphi]$. We assume that the target localization is performed using the multilateration technique that requires only the time delay measurements for target position estimation. Therefore, the complex signal amplitude and the Doppler frequency are nuisance parameters in the model considered. The parameter vector $\boldsymbol{\psi}$ for target localization in the radar network corresponds to the true target position $\boldsymbol{\psi} = \mathbf{p} = [x, y, z]$. Then the Fisher information matrix on the target position can be evaluated by applying chain rule [18]

$$\mathbf{I}(\boldsymbol{\psi}) = \mathbf{H}^T \mathbf{I}(\boldsymbol{\theta})\, \mathbf{H} \tag{19}$$

with

$$\mathbf{H} = \frac{\partial\boldsymbol{\theta}(\boldsymbol{\psi})}{\partial\boldsymbol{\psi}} = \begin{bmatrix} \frac{\partial\tau_1}{\partial x} & \frac{\partial\tau_1}{\partial y} & \frac{\partial\tau_1}{\partial z} \\ \frac{\partial\tau_2}{\partial x} & \frac{\partial\tau_2}{\partial y} & \frac{\partial\tau_2}{\partial z} \\ \vdots & \vdots & \vdots \\ \frac{\partial\tau_J}{\partial x} & \frac{\partial\tau_J}{\partial y} & \frac{\partial\tau_J}{\partial z} \end{bmatrix} \tag{20}$$

being $J \times 3$ Jacobian matrix. The detailed derivations of the Fisher information matrix for the target localization in FMCW radar network are given in Appendix A.

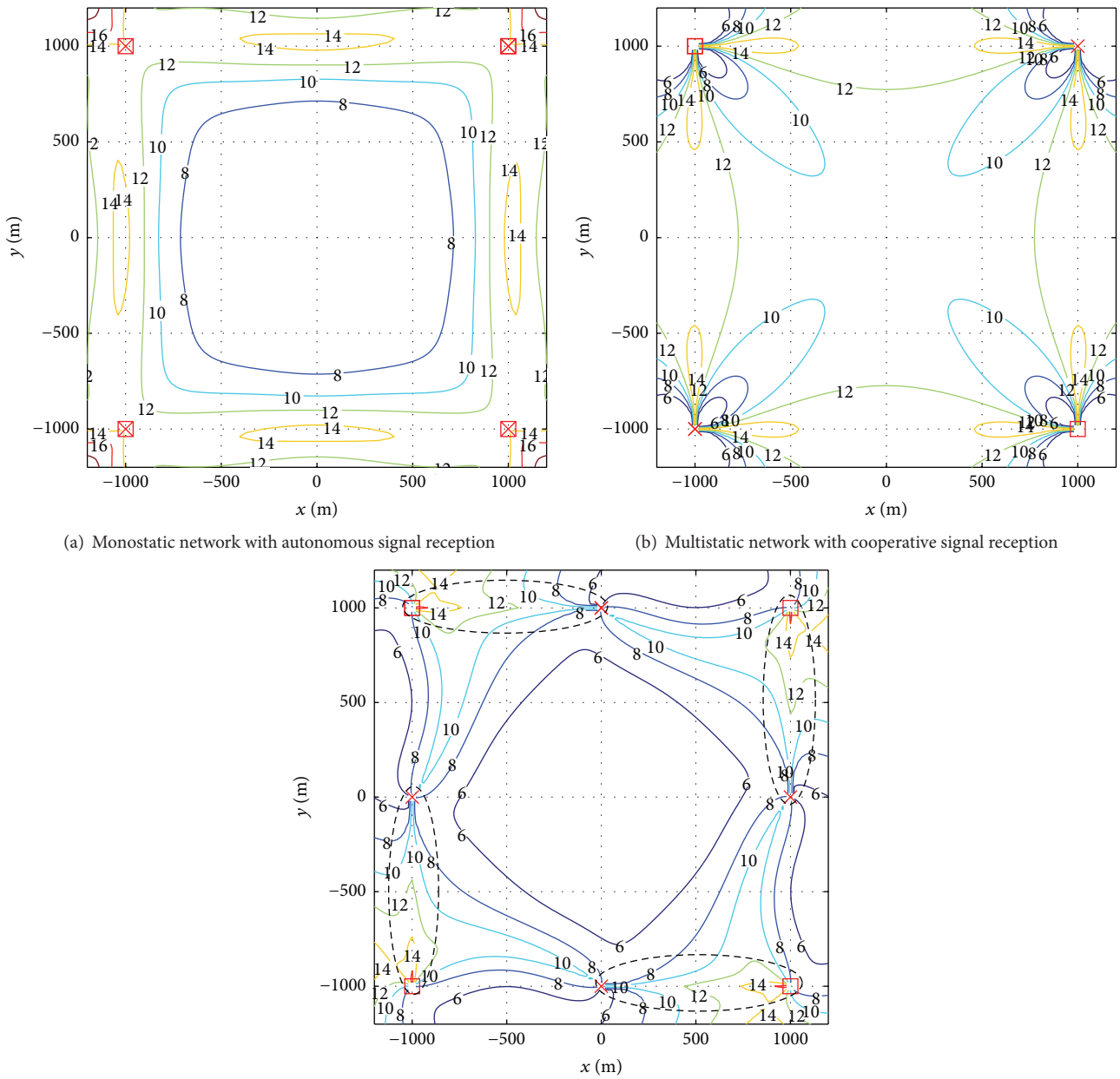

(a) Monostatic network with autonomous signal reception

(b) Multistatic network with cooperative signal reception

(c) Multistatic network with autonomous signal reception

FIGURE 2: Contours of the position estimation accuracy σ_{pos}, [m]. Red x-marks indicate positions of the transmit nodes; red squares indicate positions of the receive nodes.

4.2. The Analysis of the Potential Localization Accuracy of the Multistatic and Monostatic Radar Networks. Figure 2 shows contour plots of the target localization accuracy for three types of the FMCW radar networks with four Tx-Rx channels each, (i) monostatic radar network with autonomous mode of the signal reception (Figure 2(a)), (ii) multistatic radar network with cooperative mode of the signal reception (Figure 2(b)), and (iii) multistatic radar network with autonomous mode of the signal reception, where autonomous Tx-Rx pairs are depicted with dashed ellipses (Figure 2(c)). We define the localization accuracy as $\sigma_{\text{pos}} = \sqrt{\sigma_x^2 + \sigma_y^2}$, where σ_x^2 and σ_y^2 are variances of the estimation x and y target coordinates, respectively. The operational characteristics of single FMCW radar are given in Table 1.

The presented plots show that the multistatic network with the cooperative mode of the signal reception (Figure 2(b)) provides the equivalent localization accuracy to the monostatic radar network with autonomous mode of the signal reception (Figure 2(a)) but with two times less number of Tx-Rx channels. By introducing additional four radar nodes that form four autonomous Tx-Rx pairs of the

Table 1: Simulation parameters of a single radar node.

Parameter	Value
Transmitter power	$P_t = 25\,\text{W}$
Transmit gain	$G^{(t)} = 3.8\,\text{dBi}$
Receive gain	$G^{(r)} = 3.8\,\text{dBi}$
Processing gain	$G_p = 512 = 27.1\,\text{dB}$
Carrier frequency	$f_c = 2\,\text{GHz}$
Sweep time	$T_s = 5 \cdot 10^{-3}\,\text{s}$
Number of bursts	$N_B = 512$
Bandwidth	$\Delta f = 20\,\text{MHz}$
Receiver bandwidth	$B = 10\,\text{kHz}$
Noise figure	$F_n = 10\,\text{dB}$
Atmospheric losses	$L_{\text{amt}} = 0\,\text{dB}$
Processing losses	$L_{\text{proc}} = 0\,\text{dB}$
RF losses	$L_{\text{RF}} = 6\,\text{dB}$

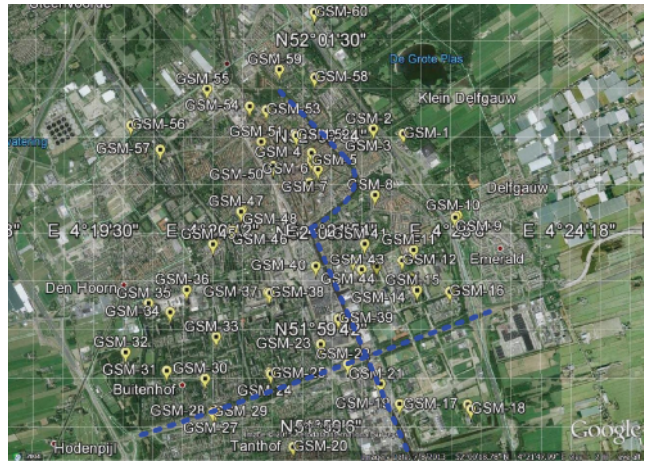

Figure 3: Positions of the GSM masts in the Delft area (blue dashed line indicates the surveillance areas).

multistatic radar network (Figure 2(c)), the localization accuracy increases, compared to the monostatic radar network (Figure 2(a)), because of the higher spatial diversity gain.

To summarize, the multisatic radar network possesses significant advantage over the monostatic radar network in terms of the localization accuracy and the number of Tx-Rx channels. This advantage can be interpreted in two ways: either as an ability to provide higher localization accuracy with the same number of Tx and Rx channels or an ability to provide the same accuracy with less number of Tx-Rx channels. Subsequently, this allows for substantial advantages in the system cost (less number of transmitting and receiving channels) compared to the monostatic radar network.

4.3. Optimization of the Multistatic Radar Network Geometry. Next, the topology optimization algorithm was applied to the scenario of the target localization in FMCW radar network along the specified areas in the city of Delft (Netherlands). These areas correspond to the canal and the highway in the city (Figure 3). The target radar cross section is RCS $= 1\,\text{m}^2$. Parameters of the single radar node are given in Table 1. The constraint on the maximum value of localization error has been set to $R_e = 5\,\text{m}$ with probability $P_e = 95\%$. The optimization algorithm has been applied for the selection of the optimal positions for transmitting and receiving radar nodes. Two scenarios of the modeling of the candidate locations for the radar nodes were considered. In the first scenario, Tx and Rx radar grids coincide and correspond to the existing locations of GSM masts (Figure 3), the coordinates of which can be found in [26], for example. In the second scenario, the nodes of the Tx radar grid correspond to the positions of the GSM masts and the nodes of the Rx radar grid are randomly generated points with mean values that correspond to the Tx grid and the standard deviation equal to 250 m. In both scenarios, the grid points of the Tx and Rx grids represent the candidate positions for the radar nodes. The reason why we consider these two scenarios is to study the effect of the spatial diversity of the Tx and Rx radar grids on the optimization result.

Figure 4 shows the distribution of the localization error around the target area of interest with optimized radar network geometry for two considered scenarios in 2D plane. For the first and the second scenarios, the maximum value of the localization error around the target area is equal to 1 m and 5 m, respectively. The number of the Tx and Rx channels is less in the second scenario due to the spatial diversity of the Tx and Rx radar units, which leads to higher signal-to-noise ratio without increasing the number of Tx-Rx channels. For the first scenario, the selected radar network includes both monostatic and bistatic radars. To summarize, the positions of the Tx and Rx grids relative to each other affect the optimization result significantly. The exploitation of the spatially separated Tx and Rx grids allows for the less number of the radar nodes required to satisfy the same accuracy constraint, compared to the scenario with fully overlapping Tx-Rx radar grids.

5. Conclusion

In this paper, the optimization approach of the multistatic radar networks with widely separated transmit and receive antennas has been developed. We have tackled the problem of the selection of the minimum number of the radars, which provide given requirements to the target localization accuracy, in the radar networks with widely separated transmitting and receiving nodes. The sparsity-based optimization approach was adopted to solve this problem. It has been shown that the optimization of the multistatic radar network geometry implies the bilinear matrix inequality problem. We have reduced this problem into the linear matrix inequality by applying the semidefinite relaxation technique. The developed framework has been applied to the geometry optimization of the FMCW multistatic radar network for the target localization. With the numerical results, it has been shown that the optimization can be performed for fully overlapping transmitting and receiving radar grids. However, setting Tx and Rx radar grids to the nonoverlapping ones results in less number of required sites for the transmission

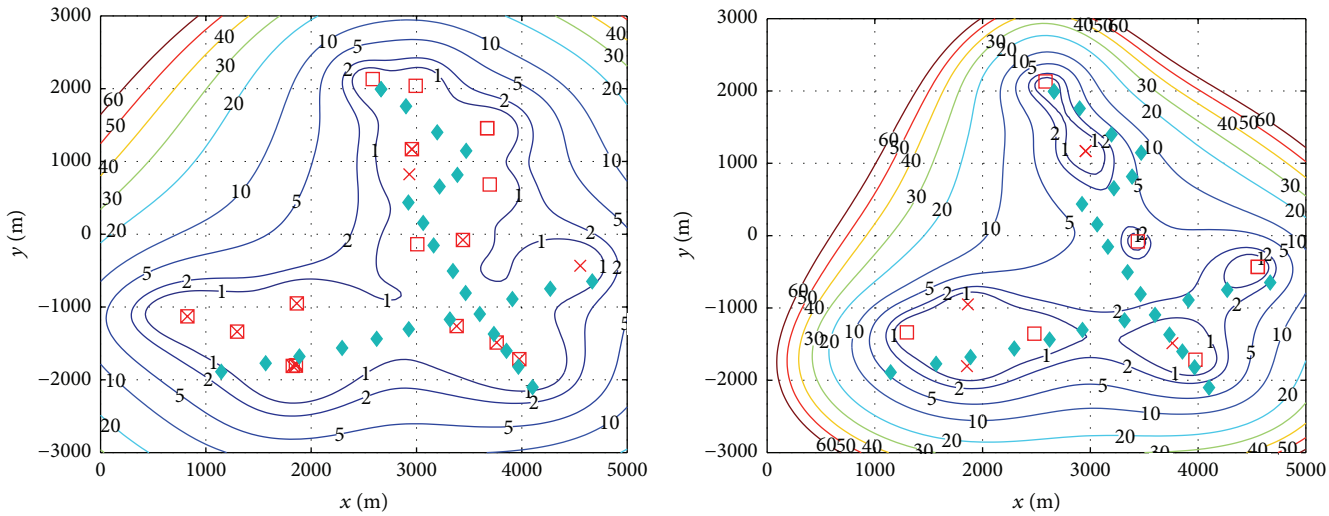

(a) Tx and Rx grids fully overlap

(b) Tx and Rx grids do not overlap

Figure 4: Contours of the position estimation accuracy σ_{pos}, [m], for optimal geometries of the radar network. Red x-marks indicate positions of the transmit nodes, red squares indicate positions of the receive nodes, and cyan diamonds correspond to target areas.

and the reception. This is due to the fact that separated Tx and Rx radar grids allow exploring the spatial diversity gain in the process of the estimation target parameters.

The proposed technique can be applied for the optimization of the radar networks that have different parameters and explore other modes of the signal reception (autonomous, cooperative, or combination of both). For example, it can be extended to the model, where the parameter vector contains other parameters, such as target velocity, or combination of different parameters, such as position and velocity vectors. Moreover, the developed framework is not limited to the estimation task; it can be applied to solve detection-driven optimization problems that arise in various types of sensors, which measure different environment parameters (temperature, pressure, humidity, etc.).

Appendix

A. The CRLB for Target Localization in the Radar Network

In FMCW radar network, the target position and velocity vectors can be extracted from the time delay or only from the Doppler frequency measurements [2, 27]. Both cases imply a two-step procedure of the 3D target localization. The first step is the estimation of the target range and radial velocity in each radar node. The second step is the estimation of the 3D target position and velocity vectors from the set of range profiles and Doppler velocities estimated locally in each radar node. Consequently, the error variances of time delay and Doppler frequency estimation $\sigma^2_{\tau\tau}$ and $\sigma^2_{\omega_d\omega_d}$ are used to evaluate the CRLB on the 3D target position and velocity vector, combining data from all radar nodes. Since in this paper we consider the problem of radar network geometry optimization for target localization, the velocity vector estimation accuracy is not analyzed here.

A.1. CRLB on the Time Delay and Doppler Frequency Estimation in the Single Radar. The Cramér-Rao Lower Bound defines the lower bound on the variance of any unbiased estimator [18, 28]. For L statistically independent signal samples $\mathbf{r} = [r_1, r_2, \ldots, r_L]$, which depend on K unknown parameters $\boldsymbol{\theta} = [\theta_1, \theta_2, \ldots, \theta_K]$, the measurement model is

$$\mathbf{r} = \mathbf{f}(\boldsymbol{\theta}) + \boldsymbol{\xi}. \tag{A.1}$$

The probability density function (PDF) of the parameter vector $\boldsymbol{\theta}$ is

$$g(\mathbf{r}; \boldsymbol{\theta}) = \prod_{l=1}^{L} \frac{1}{2\pi\sigma^2} \exp\left(-\frac{|r_l - f_l|^2}{2\sigma^2}\right), \tag{A.2}$$

where $l = 1, \ldots, L$; f_l stands for the lth noiseless reflected signal sample. The derivative of the log-likelihood function is

$$\frac{\partial \ln g}{\partial \theta_i} = \frac{1}{2\sigma^2 L} \sum_{l=1}^{L} \left[\frac{\partial f_l}{\partial \theta_i}(r_l^* - f_l^*) + \frac{\partial f_l^*}{\partial \theta_i}(r_l - f_l)\right]. \tag{A.3}$$

The received noiseless LFM signal resulting from the reflection of the target is

$$f(t) = |A| e^{i\varphi} e^{i(t-\tau)(\omega_0 + (\Delta\omega/T_s)t' - \omega_d)}, \tag{A.4}$$

where $t' = t - \tau - (q-1)T_s$.

As was discussed before, the complex signal amplitude is one of the parameters under estimation. Therefore, the FIM is given by

$$\mathbf{I} = \begin{pmatrix} I_{\tau\tau} & I_{\tau\omega_d} & I_{\tau\varphi} & I_{\tau|A|} \\ I_{\omega_d\tau} & I_{\omega_d\omega_d} & I_{\omega_d\varphi} & I_{\omega_d|A|} \\ I_{\varphi\tau} & I_{\varphi\omega_d} & I_{\varphi\varphi} & I_{\omega_d|A|} \\ I_{|A|\tau} & I_{|A|\omega_d} & I_{|A|\varphi} & I_{|A||A|} \end{pmatrix}. \tag{A.5}$$

From (6), the entries of the FIM are

$$\begin{aligned} I_{\tau\tau} &= \frac{|A|^2}{\sigma^2 L^2}\sum_{l=1}^{L}\left[\omega_0 + \frac{\Delta\omega}{T_s}t' - \omega_d\right]^2; \\ I_{\omega_d\omega_d} &= \frac{|A|^2}{\sigma^2 L^2}\sum_{l=1}^{L}(t-\tau)^2; \\ I_{|A||A|} &= \frac{1}{\sigma^2 L}; \\ I_{\varphi\varphi} &= \frac{|A|^2}{\sigma^2 L}; \\ I_{\tau\omega_d} &= \frac{|A|^2}{\sigma^2 L^2}\sum_{l=1}^{L}(t-\tau)\left[\omega_0 + \frac{\Delta\omega}{T_s}t' - \omega_d\right]; \\ I_{\tau|A|} &= 0; \\ I_{\tau\varphi} &= -\frac{|A|^2}{\sigma^2 L^2}\sum_{l=1}^{L}\left[\omega_0 + \frac{\Delta\omega}{T_s}t' - \omega_d\right]; \\ I_{\omega_d|A|} &= 0; \\ I_{\omega_d\varphi} &= -\frac{|A|^2}{\sigma^2 L^2}\sum_{l=1}^{L}(t-\tau); \\ I_{\varphi|A|} &= 0. \end{aligned} \tag{A.6}$$

Consequently, the FIM becomes

$$\mathbf{I} = \left(\begin{array}{c|c} \mathbf{G} & 0 \\ \hline 0 & I_{|A||A|} \end{array}\right), \tag{A.7}$$

where matrix $\mathbf{G}$ is

$$\mathbf{G} = \begin{pmatrix} I_{\tau\tau} & I_{\tau\omega_d} & I_{\tau\varphi} \\ I_{\omega_d\tau} & I_{\omega_d\omega_d} & I_{\omega_d\varphi} \\ I_{\varphi\tau} & I_{\varphi\omega_d} & I_{\varphi\varphi} \end{pmatrix}. \tag{A.8}$$

The inverted FIM is

$$\mathbf{I}^{-1} = \left(\begin{array}{c|c} \mathbf{G}^{-1} & 0 \\ \hline 0 & \dfrac{1}{I_{|A||A|}} \end{array}\right), \tag{A.9}$$

which follows from

$$\mathbf{I}^{-1} = \left(\begin{array}{c|c} \mathbf{G}\mathbf{G}^{-1} & 0 \\ \hline 0 & I_{|A||A|}\dfrac{1}{I_{|A||A|}} \end{array}\right) = \left(\begin{array}{c|c} \mathbb{1} & 0 \\ \hline 0 & 1 \end{array}\right). \tag{A.10}$$

The variance of the time delay measurement errors is

$$\begin{aligned} \sigma_{\tau\tau}^2 &= \left[\mathbf{I}^{-1}\right]_{\tau\tau} = \left[\mathbf{G}^{-1}\right]_{\tau\tau} \\ &= \frac{1}{\det(\mathbf{G})}\left[I_{\omega_d,\omega_d}I_{\varphi,\varphi} - I_{\varphi,\omega_d}^2\right]. \end{aligned} \tag{A.11}$$

Using the Taylor series expansion, we can derive the closed-form expression for $\sigma_{\tau\tau}^2$:

$$\sigma_{\tau\tau}^2 \approx \frac{3}{2}\frac{1}{\Delta\omega^2 \mathrm{SNR}}, \tag{A.12}$$

where the SNR is defined as $\mathrm{SNR} = |A|^2/2\sigma^2$.

A.2. CRLB on the Target Position Estimation in Radar Network. The parameter vector of 3D target position estimation in the radar network is $\boldsymbol{\psi} = [x, y, z]$. According to [18], entries of the Fisher information matrix are

$$I_{ij} = \sum_{l=1}^{L}\frac{\partial f_l}{\partial \psi_i}\frac{1}{\sigma_l^2}\frac{\partial f_l}{\partial \psi_j}, \tag{A.13}$$

where f_l is a function that relates measured lth parameter with the parameter under estimation and L is the total number of measurements; $i = 1, \ldots, K$; $j = 1, \ldots, K$. The number of measurements (time delays) L in the radar network, associated with one target, is equal to the number of radars J. We rewrite (A.13) as

$$I_{ij} = \sum_{l=1}^{J}\frac{\partial \tau_l}{\partial \psi_i}\frac{1}{(\sigma_{\tau\tau}^2)^{(l)}}\frac{\partial \tau_l}{\partial \psi_j}, \tag{A.14}$$

where τ_l is the signal time delay measured in lth bistatic radar (2); $(\sigma_{\tau\tau}^2)^{(l)}$ is the variance of the time delay estimation in the lth radar. The derivatives $\partial\tau_l/\partial\psi_i$ from (A.14) are

$$\begin{aligned} \frac{\partial \tau_l}{\partial x} &= \frac{1}{c}\left(\frac{x - x_n^{(t)}}{R_n^{(t)}} + \frac{x - x_m^{(r)}}{R_m^{(r)}}\right); \\ \frac{\partial \tau_l}{\partial y} &= \frac{1}{c}\left(\frac{y - y_n^{(t)}}{R_n^{(t)}} + \frac{y - y_m^{(r)}}{R_m^{(r)}}\right); \\ \frac{\partial \tau_l}{\partial z} &= \frac{1}{c}\left(\frac{z - z_n^{(t)}}{R_n^{(t)}} + \frac{z - z_m^{(r)}}{R_m^{(r)}}\right). \end{aligned} \tag{A.15}$$

Conflict of Interests

The authors declare that there is no conflict of interests regarding the publication of this paper.

Acknowledgments

This work has been partly performed within the RAEBELL project. The authors would like to thank Geert Leus, Sundeep Prabhakar Chepuri, Jonathan Bosse, and Ronny I. A. Harmanny for fruitful discussions.

References

[1] D. Pepyne, D. McLaughlin, D. Westbrook et al., "Dense radar networks for low-flyer surveillance," in *Proceedings of the 11th IEEE International Conference on Technologies for Homeland Security (HST '11)*, pp. 413–418, IEEE, Waltham, Mass, USA, November 2011.

[2] E. Anniballi, D. Petri, A. Yarovoy, and O. Krasnov, "Active radar networks for terminal security airport," in *Proceedings of the 15th International Radar Symposium (IRS '14)*, pp. 1–4, Gdansk, Poland, June 2014.

[3] A. Di Lallo, A. Farina, R. Fulcoli, A. Stile, L. Timmoneri, and D. Vigilante, "A real time test bed for 2D and 3D multi-radar tracking and data fusion with application to border control," in *Proceedings of the CIE International Conference on Radar (ICR '06)*, pp. 1–6, IEEE, Shanghai, China, October 2006.

[4] J. Li and P. Stoica, *MIMO Radar Signal Processing*, Wiley and Sons, New York, NY, USA, 2008.

[5] I. Ivashko, O. Krasnov, and A. Yarovoy, "Performance analysis of multisite radar systems," in *Proceedings of the 10th European Radar Conference (EuRAD '13)*, pp. 459–462, IEEE, Nuremberg, Germany, October 2013.

[6] D. J. Torrieri, "Statistical theory of passive location systems," *IEEE Transactions on Aerospace and Electronic Systems*, vol. 20, no. 2, pp. 183–198, 1984.

[7] J. Isaacs, D. Klein, and J. Hespanha, "Optimal sensor placement for time difference of arrival localization," in *Proceedings of the 48th IEEE Conference on Decision and Control, 28th Chinese Control Conference (CDC/CCC '09)*, pp. 7878–7884, Shanghai, China, December 2009.

[8] H. Godrich, A. M. Haimovich, and R. S. Blum, "Target localization accuracy gain in MIMO radar-based systems," *IEEE Transactions on Information Theory*, vol. 56, no. 6, pp. 2783–2803, 2010.

[9] A. A. Gorji, T. Kirubarajan, and R. Tharmarasa, "Antenna allocation for MIMO radars with collocated antennas," in *Proceedings of the 15th International Conference on Information Fusion (FUSION '12)*, pp. 424–431, IEEE, Singapore, September 2012.

[10] J. Ranieri, A. Chebira, and M. Vetterli, "Near-optimal sensor placement for linear inverse problems," *IEEE Transactions on Signal Processing*, vol. 62, no. 5, pp. 1135–1146, 2014.

[11] S. P. Chepuri and G. Leus, "Sparsity-promoting sensor selection for non-linear measurement models," *IEEE Transactions on Signal Processing*, vol. 63, no. 3, pp. 684–698, 2015.

[12] M. Al-Obaidy, A. Ayesh, and A. F. Sheta, "Optimizing the communication distance of an ad hoc wireless sensor networks by genetic algorithms," *Artificial Intelligence Review*, vol. 29, no. 3-4, pp. 183–194, 2008.

[13] I. M. Ivashko, O. A. Krasnov, and A. G. Yarovoy, "Receivers topology optimization of the combined active and WiFi-based passive radar network," in *Proceedings of the 11th European Radar Conference (EuRAD '14)*, pp. 517–520, Rome, Italy, October 2014.

[14] M. Svecová, D. Kocur, and R. Zetik, "Object localization using round trip propagation time measurements," in *Proceedings of the 18th International Conference in Radioelektronika*, pp. 1–4, IEEE, Prague, Czech Republic, April 2008.

[15] M. Radmard, S. M. Karbasi, and M. M. Nayebi, "Data fusion in MIMO DVB-T-based passive coherent location," *IEEE Transactions on Aerospace and Electronic Systems*, vol. 49, no. 3, pp. 1725–1737, 2013.

[16] Q. He, R. S. Blum, H. Godrich, and A. M. Haimovich, "Target velocity estimation and antenna placement for MIMO radar with widely separated antennas," *IEEE Journal on Selected Topics in Signal Processing*, vol. 4, no. 1, pp. 79–100, 2010.

[17] Q. He, R. S. Blum, and A. M. Haimovich, "Non-coherent MIMO radar for target estimation: more antennas means better performance," in *Proceedings of the 43rd Annual Conference on Information Sciences and Systems (CISS '09)*, pp. 108–113, IEEE, Baltimore, Md, USA, March 2009.

[18] S. Kay, *Fundamentals of Statistical Signal Processing: Estimation Theory*, vol. 1 of *Prentice Hall Signal Processing Series*, Prentice Hall, New York, NY, USA, 1993.

[19] J. Helferty and D. R. Mudgett, "Optimal observer trajectories for bearings only tracking by minimizing the trace of the cramer-rao lower bound," in *Proceedings of the 32nd IEEE Conference on Decision and Control*, vol. 1, pp. 936–939, San Antonio, Tex, USA, December 1993.

[20] S. Joshi and S. Boyd, "Sensor selection via convex optimization," *IEEE Transactions on Signal Processing*, vol. 57, no. 2, pp. 451–462, 2009.

[21] F. Gustafsson and F. Gunnarsson, "Mobile positioning using wireless networks: possibilities and fundamental limitations based on available wireless network measurements," *IEEE Signal Processing Magazine*, vol. 22, no. 4, pp. 41–53, 2005.

[22] E. Cands, M. Wakin, S. Boyd, and E. Cands, "Enhancing sparsity by reweighted 1 minimization," *Journal of Fourier Analysis and Applications*, vol. 14, no. 5-6, pp. 877–905, 2008.

[23] S. Boyd and L. Vandenberghe, "Semidefinite programming relaxations of non-convex problems in control and combinatorial optimization," in *Communications, Computation, Control and Signal Processing: A Tribute to Thomas Kailath*, A. Paulraj, V. Roychowdhuri, and C. Schaper, Eds., pp. 279–288, Kluwer, 1997.

[24] A. d'Aspremont and S. Boyd, "Relaxations and randomized methods for nonconvex QCQPs," EE392o Class Notes, 2003.

[25] G. Babur, O. A. Krasnov, A. Yarovoy, and P. Aubry, "Nearly orthogonal waveforms for MIMO FMCW radar," *IEEE Transactions on Aerospace and Electronic Systems*, vol. 49, no. 3, pp. 1426–1437, 2013.

[26] Waar staan de gsm en umts masten in nederland?, http://www.gsmmasten.nl.

[27] I. Shames, A. N. Bishop, M. Smith, and B. D. O. Anderson, "Doppler shift target localization," *IEEE Transactions on Aerospace and Electronic Systems*, vol. 49, no. 1, pp. 266–276, 2013.

[28] H. Van Trees, *Detection, Estimation, and Modulation Theory*, Detection, Estimation, and Filtering Theory, part 1, Wiley, New York, NY, USA, 2nd edition, 2004.